

**DETC2011-PTG48824**

## **MACHINING AND RUNNING TEST OF HIGH-PERFORMANCE FACE GEAR SET**

**Isamu Tsuji**

IWASA TECH  
4-5-4 Shinkiba, Koutouku, Tokyo  
136-0082, Japan

**Kazumasa Kawasaki**

Niigata University  
8050 Ikarashi 2-nocho, Nishi-ku, Niigata  
950-2181, Japan

**Hiroshi Gunbara**

Matsue National College of Technology  
14-4 Nishi-Ikuma Cho, Matsue, Shimane  
690-8518, Japan

**Akiyasu Takami**

Matsue National College of Technology  
14-4 Nishi-Ikuma Cho, Matsue, Shimane  
690-8518, Japan

### **ABSTRACT**

The purpose of this research is to develop a high-performance face gear set for aircraft. The geometrical design method of the face gear has already been proposed, and how to decide an effective engagement area under the design parameter has been clarified. A numerical example is presented based on the proposed method. Before machining test, the modified-tooth was decided by the developed Tooth Contact Analysis (TCA) program in order to control the tooth contact pattern. The influence of alignment error of each axis of gear was investigated using TCA. The designed modified-tooth was processed by the Multi-Tasking machine. Finally, running test was performed at a pinion rotating speed of 970 rpm. The face gear set can be operated continuously at an maximum load torque 1390 N · m, without any trouble. The transmission efficiency reached 98.9% under maximum load torque. This cutting method of the face gear introduces a new degree of freedom for defining optional shapes of tooth modification.

### **1 INTRODUCTION**

In the power transmission system of automobile and aircraft, bevel gears and hypoid gears are the most common gears used for power transmission between intersecting and nonintersecting-nonparallel shafts. Recently, the trial which has intended to use the face gears instead of these gears has begun, and the example applied to the torque split mechanism of the helicopter has been coming out [1]. The advantage utilizing face gears is to achieve the lightweight transmitting two gears by only one pinion. Hereafter, the possibility of a lot of applications utilizing cylindrical pinion is expected. For this

reason, design, analysis of tooth contact and FEM, and manufacturing of face gears have been tried by many researchers [2-8].

The geometrical design method of the face gear has already been proposed, and how to decide an effective engagement area under the design parameters have been clarified [9, 10]. The face gear has two unique dimensions which control the face width of the teeth, the outer and inner diameter of the face gear. These two parameters can be provided by the new geometrical design method, and the method is applied to the design of the face gear with a spur gear as pinion. However, the problem remains in the practical use of the face gear. It is how to avoid the influence of machining and assembly errors on tooth contact pattern. Generally, the conventional method which modifies tooth profile of pinion is used to control the influence of machining and assembly errors on tooth contact pattern. However, it is hard to control tooth contact pattern intentionally and position of pinion axis has to adjust as assembling in this method. In this paper, a new method which modifies gear tooth surface is proposed on condition that the hardened gear-teeth finishing process can be carried out using the general-purpose Multi-Tasking machine. A numerical example of the influence of the assembly errors was presented based on the proposed method using TCA [11]. The face gear with modified tooth surface was machined using Multi-Tasking machine. For this machining, first the numerical coordinates on the tooth surfaces of the face gear is calculated and the tooth profiles is modeled using a 3D-CAD system. The material of the work-piece was SCM420 and it was machined by cutting using a coated carbide ball end mill. After rough cutting, face gear tooth surface was



axis. That means the pinion is rotated by  $\theta$ . In this condition, the transverse profile of the pinion with right-hand teeth at  $z_1=v$  is shown in Fig. 3 assuming that distance from transverse plane in center of face width. A point P on the right flank of the transverse tooth profile is represented by  $\mathbf{r}$  in the coordinate system  $O-xyz$ . Using  $\phi$  which denotes comprehensively 3 values  $\theta, u$ , and  $\eta_b$  with regard to rotation around the pinion axis,  $\mathbf{r}$  and tooth surface unit normal  $\mathbf{n}$  on the point P are represented by Eq. (2):

$$\mathbf{r} = \begin{bmatrix} x\{\phi(u;\theta)\} \\ y\{\phi(u;\theta)\} \\ z(v) \end{bmatrix} = \begin{bmatrix} \pm r_b(\sin\phi - u\cos\phi) \\ r_b(\cos\phi + u\sin\phi) \\ v \end{bmatrix}, \quad \mathbf{n} = \begin{bmatrix} \pm \cos\phi \\ -\sin\phi \\ 0 \end{bmatrix} \quad (2)$$

where  $\phi$  is represented by Eq. (3):

$$\phi = u + \eta_b \mp \theta \quad (3)$$

Hereafter, the right tooth flank is examined. The velocities of pinion and gear on the point P are defined as  $\mathbf{v}_1$  and  $\mathbf{v}_2$ , respectively. The relative velocity of the gear for the pinion on the point P is defined as  $\mathbf{w} = \mathbf{v}_1 - \mathbf{v}_2$ , and  $\mathbf{w}$  is represented by Eq. (4):

$$\frac{\mathbf{w}}{\omega_2} = \begin{bmatrix} v + ir_b(\cos\phi + u\sin\phi) \\ -ir_b(\sin\phi - u\cos\phi) \\ e - r_b(\sin\phi - u\cos\phi) \end{bmatrix} \quad (4)$$

When the value  $u$  is given,  $v$  which satisfies the contact condition  $\mathbf{n} \cdot \mathbf{w} = 0$  is defined as  $v^*$ .  $v^*$  is represented by Eq. (5):

$$v^* = -\frac{i \cdot r_b}{\cos\phi} \quad (5)$$

When the pinion is rotated by  $\theta$  from its standard rotational position, the contact point  $\mathbf{r}^*$  represented in the coordinate system  $O-xyz$  is given by Eq. (6). It is possible to obtain the coordinate of the contact point  $\mathbf{r}^*$  by replacing  $v$  of Eq. (1) with  $v^*$ . The contact line can be obtained by continuously changing  $u$ :

$$\mathbf{r}^* = \begin{bmatrix} x^* \\ y^* \\ z^* \end{bmatrix} = \begin{bmatrix} r_b(\sin\phi - u\cos\phi) \\ r_b(\cos\phi + u\sin\phi) \\ -i \cdot r_b / \cos\phi \end{bmatrix} \quad (6)$$

Considering  $\mathbf{r}_2^*$  which converted  $\mathbf{r}^*$  into the  $O-x_1y_1z_1$  coordinate system, it is possible to obtain contact lines appearing on the gear tooth flank.

$$\mathbf{r}_2^* = \begin{bmatrix} x_2(u;\theta) \\ y_2(u;\theta) \\ z_2(u;\theta) \end{bmatrix} = \begin{bmatrix} (e-x)\cos(\theta/i) + v^*\sin(\theta/i) \\ (e-x)\sin(\theta/i) - v^*\cos(\theta/i) \\ r_p - y \end{bmatrix} \quad (7)$$

### 3 EFFECTIVE ENGAGEMENT AREA

In the gear performance, meshing trouble of tooth engagement getting stuck could come up [12]. Therefore, the effective diameter of the face gear at the inner end is limited by this trouble. In the face gear performance, it is necessary to consider two meshing troubles to be discussed below.

One is the particular points on the pinion flank, where meshing engagement gets stuck. On the points specific sliding of the pinion becomes  $-\infty$ . The pinion part beyond the line of the points, where contact lines don't appear, doesn't work well as tooth flank.

The other trouble is the particular points on the gear tooth flank, where meshing engagement gets stuck. On the points specific sliding of the gear becomes  $-\infty$ . The gear part beyond the line of the points is undercut by the tip of tooth of pinion.

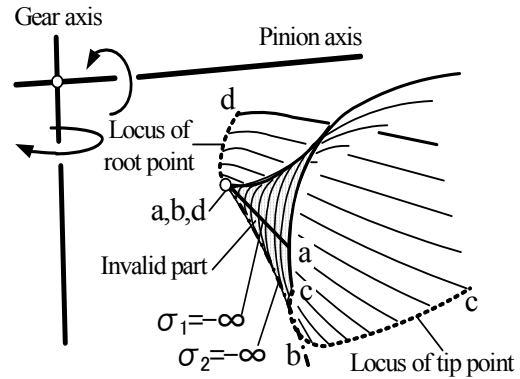


Figure 4. Surface of action

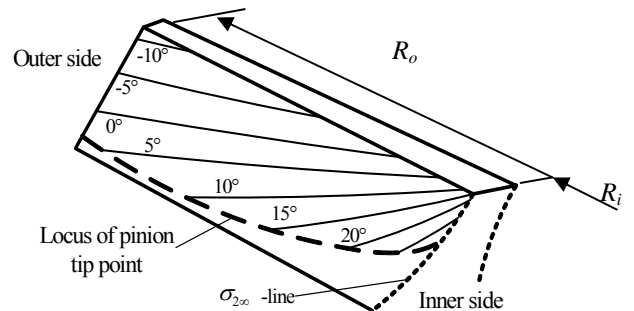


Figure 5. Contact lines on the gear tooth flank

**Table 1.** Design data of face gear

Shaft angle (deg.)	90	Offset (mm)	0
Normal Module(mm)	2.54	Pressure angle (deg.)	20
Pinion		Face Gear	
Number of teeth	25	Number of teeth	120
P.C.D.(mm)	63.5	Addendum (mm)	2.54
Profile shift coeff.	0	Dedendum (mm)	3.175
Outer dia.(mm)	68.58	Tooth tip thick.(mm)	1
Root dia.(mm)	58.42	Inner end dia. (mm)	282
Base circle dia.(mm)	57.5505	Outer end dia. (mm)	342
Circular tooth thick.(mm)	3.99		

The design data for an example of a face gear set is shown in Table 1.

The surface of action of the face gear is shown in Fig. 4. The area surrounded from  $\sigma_2$ -line (b-b) and locus of tip and root points of pinion (c-c, d-d) becomes the effective meshing region. The part which conducted the sandy pattern shows the invalid meshing region.

Contact lines appearing on the gear tooth surface are shown in Fig. 5. The numerical value appended to each contact line shows rotation angle of the pinion. In the gear design, the inner end radius  $R_i$  of gear is decided so that the effective meshing region may not contain the  $\sigma_2$ -line. The outer end radius  $R_o$  of gear is decided so that the tooth tip thickness becomes about 1 mm.

#### 4 MODIFIED TOOTH FLANK

For all kinds of gear, tooth surface modifications are usually used to control the tooth contact pattern up to the usage of gear. There are two ways to modify the flank. One is the modification of pinion flank, another is gear flank. Modification of pinion flank is more conventional than gear, for example just applying usual crowning of tooth width direction and circular modification of tooth profile.

In this paper, new method which modifies gear tooth surface is proposed on condition that the hardened gear-teeth finishing process can be carried out using the general-purpose M u l t i -

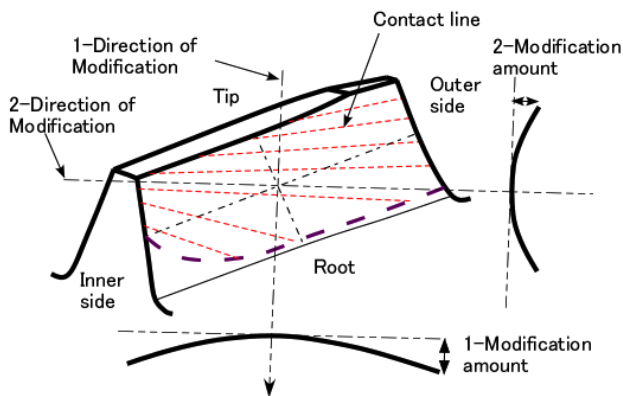


**Figure 6.** Tooth profile modification

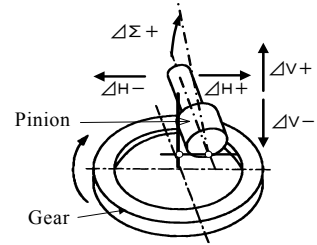


**Figure 7.** Assembly error and gear shaft angle error

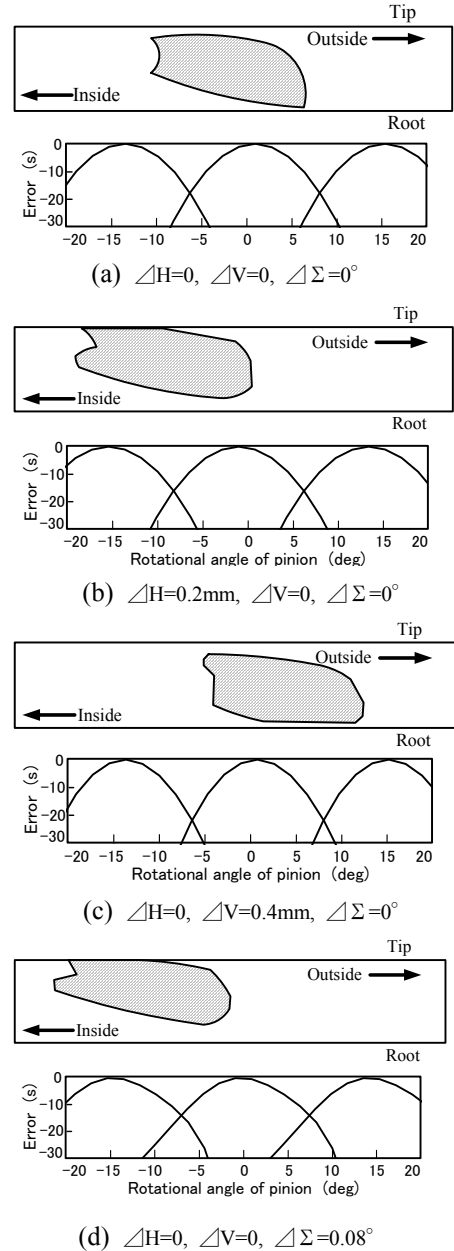


**Figure 8.** Results of tooth contact analysis

Tasking machine and ball end mill. Figure 6 shows each contact lines appearing on the gear tooth flank having tilting angle to the face width direction of gear. Curved modifications of two different directions are applied to gear flank. One is parallel to the contact line that goes through the center of tooth flank, another is rectangular. The amount and direction for each modification can be changed independently.

The influence of machining and assembly errors on tooth contact pattern was investigated using TCA [11]. In order to calculate the assembly condition, the following are defined. If the designing axes of the pinion and gear axes coincide with each other and the shaft angle is equal to the design value, this position of the face gear is named the regular one. Figure 7 shows the assembly and shaft angle errors. If the gear is fixed, the assembly errors  $\Delta H$  and  $\Delta V$  are defined as the deviations of the pinion in  $H$  and  $V$  directions from the regular position, and also the shaft angle error  $\Delta\Sigma$  is defined as the difference from the regular shaft angle.

Figure 8 shows the tooth contact pattern on the gear tooth and transmission error of face gear with modification of gear tooth surface. These results are obtained by TCA calculation. The modification of gear tooth surface was given to get a proper tooth contact pattern. When the assembly error is not given (a), the size of tooth contact pattern is about 40 % of tooth width and 70 % of tooth profile. In Fig. 8, (b) to (d) are the results when the assembly error expected practically are given. Every tooth contact pattern moves inside of tooth surface without edge contact. The transmission errors are also good condition. As a result, the validity of this modification method is confirmed.

## 5 MACHINING TEST

In the previous section, the gear tooth surface was modified appropriately using TCA and the numerical coordinates on the gear tooth surface and normal vectors were calculated. Figure 9 shows tooth profile of face gear modeled using a 3D-CAD system based upon the calculated numerical coordinates. The shape of the root is flat and corner is 0.75 mm radius.

Tool passes in Fig. 10 are set up automatically after checking tool interferences, choosing end mill. Face gear was machined by a ball end mill (R0.75 mm) utilizing a vertical

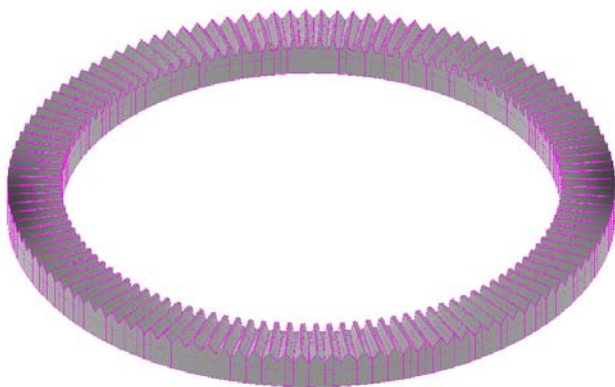


Figure 9. CAD-model

machining center (Makino V99) with 3-axis for CNC milling machine. A ball end mill (R0.75 mm) made of cemented carbide with special coating for a hard cutting tool was used in cutting hardened tooth surface. Cutting speed was 400 mm/min. and feed was 0.1 mm. The pitch of cutting depth was 0.1 mm. Tooling was changed one time by automatic tooling changer while finishing tooth surface. Any unusual wear of tooling was not observed.

Figure 11 shows machining of face gear on 3-D vertical machining center. The machined face gear surface was measured using a coordinate measuring machine [13, 14]. Figure 12 shows the measured result. Straight dotted lines are nominal data without any modification. Thick curved lines are measured results [ $\mu\text{m}$ ] after machining. Gear tooth spacing and runout errors was within AGMA 10 class. The surface roughness was Ra 0.5-0.6  $\mu\text{m}$ . As a result, the gear tooth surface was machined intentionally and it was proved that machining was done appropriately.

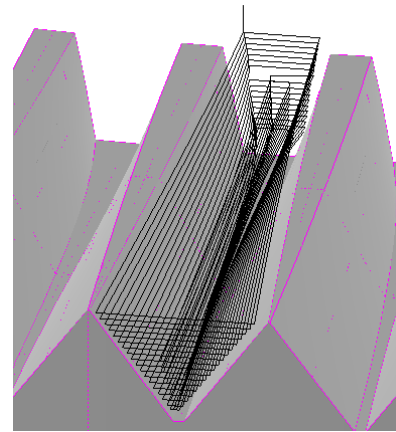
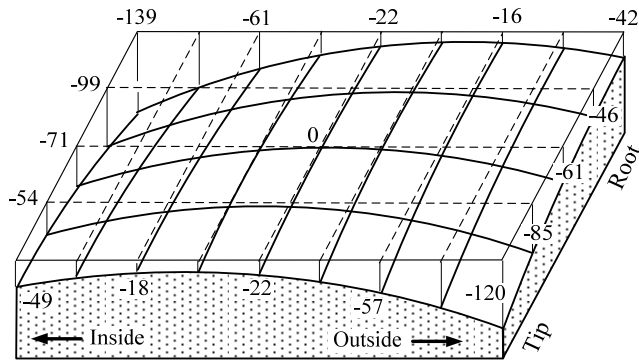


Figure 10. Tool passes



Figure 11. Machining of face gear



**Figure 12.** Result of tooth shape measurement



**Figure 13.** Face gear set on meshing tester

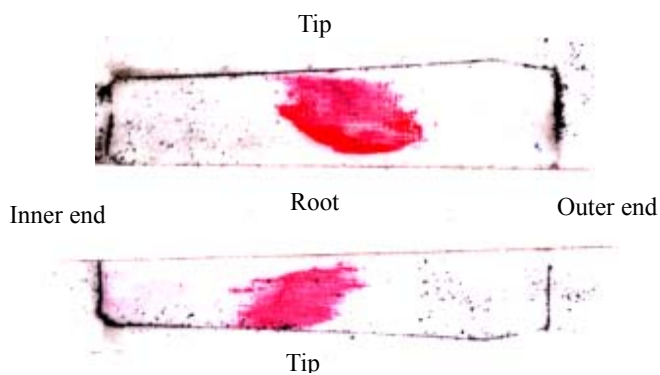


**Figure 14.** Results of tooth contact pattern test

The tooth contact pattern was also checked on the meshing tester in Fig. 13. Figure 14 shows the actual tooth contact pattern. As a result, it was very resemble to the result of TCA in Fig. 8 (a).

## 6 RUNNING TEST

Figure 15 shows the experimental device for full-load running test. The input shaft was turn by 45 kw DC motor.

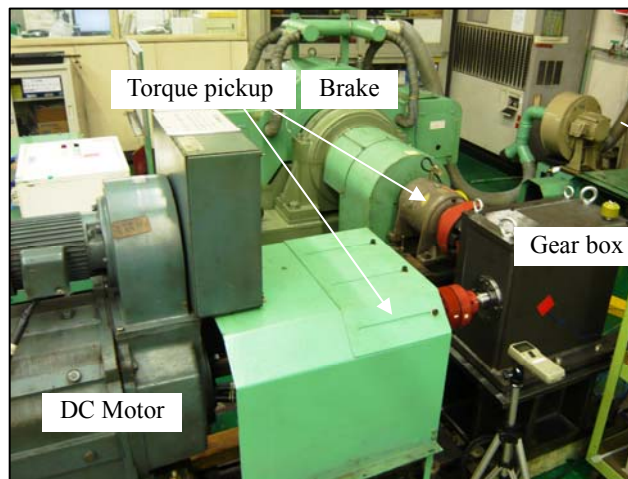


**Figure 15.** Experimental device

The output shaft was joined to brake and torque was applied to a gear box. Torque pike-up meters were set up to the input and output shafts and transmission efficiency of face gear assembled in gear box was found by measuring torsional torque. The temperature of gear box and lubrication oil was measured by thermocouples put on the outside and inside of gear box. Running test was performed by 4 steps of loaded torque that were changed gradually from 348 N · m (25%), 695 N · m (50%), 1043 N · m (75%) to 1390 N · m (maximum torque 100%). For each load, running test was finished when rising amount of oil temperature was less than 0.5° for 30 minutes. A number of revolution of input shaft was 970 rpm. Results of running test of 25% and 100% were represented graphically as shown in Fig. 13. The vertical axis shows transmission efficiency and oil temperature, and the horizontal axis shows running time. In these graphs, CW means clock wise direction and CCW means counter clock wise direction of revolution of input shaft. The oil temperature was compensated by subtracting room temperature.

Rapid rising of temperature were not observed for each tests and transmission efficiency finally reached 98.9% for CW condition.

Figure 17 shows the tooth contact pattern on gear tooth surface after 100% running test. Before running test, the gear tooth surface was painted. Afterwards, 100% running test was performed. Shining area peeled off the paint on the gear tooth surface was actual tooth contact pattern under 100% running test. Comparing with tooth contact pattern of no-load meshing test, tooth contact pattern of full-load running test spread, especially toward inner side. Any damage or partial strong contact was not observed on the gear tooth surface.

From these results, the validity of proposed modification method of gear tooth and machining method were confirmed. Face gear machined in this paper had enough durability for the actual application.

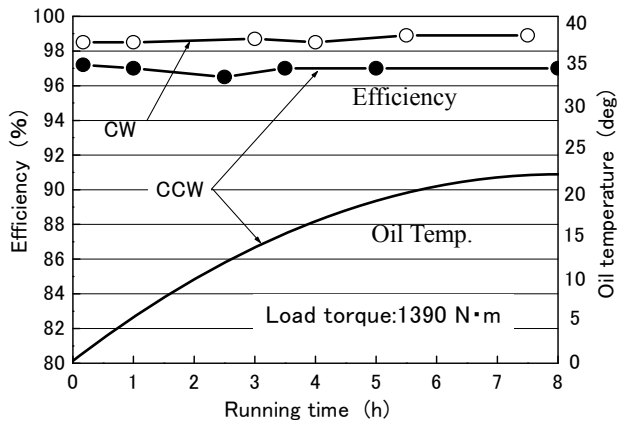
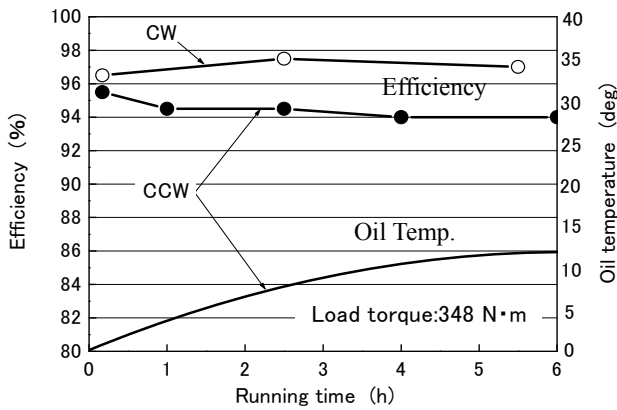


Figure 16. Efficiency and oil

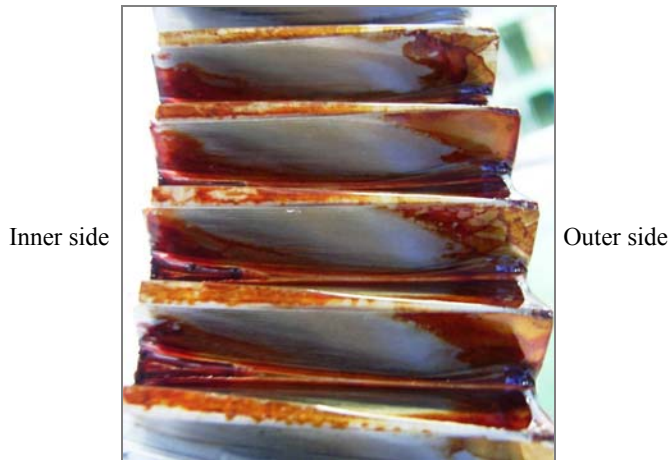


Figure 17. Tooth contact patterns after running test

## 7 CONCLUSIONS

The high-performance face gear set was developed in this paper. Trial machining and running test of this face gear set was done. First, basic design parameters were decided according with the design method that authors had already proposed. Next,

a new modification method of gear tooth surface was applied using TCA program. A face gear with gear tooth surface hardened by carburizing was machined using 3D vertical machining center. Afterwards, the gear tooth surface was measured and tooth contact pattern was checked on meshing tester. As a result, it was confirmed that face gear was machined in high accurate. In addition, the result of running test was that transmission efficiency reached 98.9% for CW condition under loaded torque 1390 N·m. It was proved that face gear set machined in this paper had enough capability of the power transmission for the actual application.

## 8 NOMENCLATURE

- $A_1$  = Pinion axis
- $E$  = Common perpendicular of pinion and gear shafts
- $e$  = Offset quantity between pinion and gear shafts
- $\omega_1, \omega_2$  = Angular velocity of pinion and gear, respectively
- $z_1, z_2$  = Number of teeth of pinion and gear, respectively
- $m$  = Module
- $\alpha$  = pressure angle
- $\chi$  = Addendum modification coefficient
- $i$  = Gear ratio
- $r_b$  = Radius of base cylinder
- $u$  = Involute roll angle which determines transverse profile
- $\eta_b$  = Space width half angle
- $\theta$  = Rotation angle of  $O_1-x_1y_1z_1$  around pinion axis
- $v$  = Distance from transverse plane in center of face width
- $r$  = Coordinates of point P on right flank of transverse tooth profile
- $n$  = Unit normal vector of  $r$
- $v_1, v_2$  = Velocity of pinion and gear, respectively
- $w$  = Relative velocity of gear for pinion
- $v^*$  =  $v$  which satisfies contact condition
- $r^*$  =  $r$  which satisfies contact condition
- $R_i$  = Inner end radius
- $R_o$  = Outer end radius
- $\Delta H$  = Horizontal assembly error
- $\Delta V$  = Vertical assembly error
- $\Delta \Sigma$  = Shaft angle error

## 9 REFERENCES

- [1] Litvin, F. L., et al., 1992, Application of Face-Gear Drives in Helicopter Transmissions, Proc. of the 1992 International Power Transmissions and Gearing Conference, ASME, pp.267-274.
- [2] Handschuh, R. F., Lewicki D. G., Heath G. F. et al, 1996, Experimental Evaluation of Face Gears for Aerospace Drive System Applications, Proc. of the 7th Int. Power Transmissions and Gearing Conference, San Diego, California, pp.581-587.
- [3] Zhang Y. and Wu Z., 1997, Offset Face Gear Drives: Tooth Geometry and Contact Analysis, Trans. ASME, Journal of Mechanical Design, Vol. 119, pp. 114-119.

- [4] Litvin F. L., Fuentes A., Zanzi C., Pontiggia, M., and Handschuh, R. F., 2002, Face-gear Drive with Spur Involute Pinion: Geometry, Generation, by a Worm, Stress Analysis, *Comput. Methods Appl. Mech. Engrg.*, 191, pp. 2785-2813.
- [5] Moriwaki I, Ogaya S., and Watanabe K., 2003, Stress Analysis of Face Gear Tooth Subject to Distributed Load Using Global Local Finite Element Method (GLFEM), *Proc. of the ASME Design Engineering Technical Conferences*, Chicago, pp. 289-296.
- [6] Tan J., 2003, Face Gearing with a Conical Involute Pinion. Part 2. The Face Gear-meshing with the Pinion, Tooth Geometry, and Generation, *Proc. of the ASME Design Engineering Technical Conferences*, Chicago, pp. 687-692.
- [7] Guingand M., Vaujany J. D., and Jacquin C., 2005, Quasi-static Analysis of a Face Gear under Torque, *Comput. Methods Appl. Mech. Engrg.*, 194, pp. 4301-4318.
- [8] Ohshima F., and Yoshino H., 2006, Study on High Reduction Face Gears, *Transactions of the Japan Society of Mechanical Engineers, Series C, Vol. 72, No.720*, pp.2672-2682 (in Japanese).
- [9] Gunbara, H., 2007, Geometrical Design of Face gear, *Transactions of the Japan Society of Mechanical Engineers, Series C, Vol. 73, No.726*, pp.589-593 (in Japanese).
- [10] Gunbara, H. and Kawasaki, K., 2008, Geometrical Design of Point-Contact Face Gear, *Transactions of the Japan Society of Mechanical Engineers, Series C, Vol. 74, No.745*, pp.197-201 (in Japanese).
- [11] Stadtfeld, H. J., 1993, *Handbook of Bevel and Hypoid Gears*, Rochester Institute of Technology, R.I.T., pp.9-12.
- [12] Naruse, M. et al, 1960, A Study of Gear, pp. 77-170, Youkendo Co. Ltd. (in Japanese).
- [13] Fan, Q, Ronald DaFoe S., and W.Swanger Jiohn, 2008, High – Order Tooth Flank Form Error Correction for Face-Milled Spiral Bevel and Hypoid Gears, *Journal of Mechanical Design*, Vol.130/072601-1.
- [14] Stadtfeld, H. J., 2000, *Advanced Bevel Gear Technology for The New Millennium*, Edition.